

Tissue-specific Autophagy Alterations and Increased Tumorigenesis in Mice Deficient in Atg4C/Autophagin-3*

Received for publication, February 8, 2007, and in revised form, March 21, 2007. Published, JBC Papers in Press, April 17, 2007, DOI 10.1074/jbc.M701194200

Guillermo Mariño[‡], Natalia Salvador-Montoliu[‡], Antonio Fueyo[§], Erwin Knecht[¶], Noboru Mizushima^{||}, and Carlos López-Otín^{‡1}

From the [‡]Departamento de Bioquímica y Biología Molecular and [§]Biología Funcional, Facultad de Medicina, Instituto Universitario de Oncología, Universidad de Oviedo, 33006 Oviedo, Spain, [¶]Laboratorio de Biología Celular, Centro de Investigación Príncipe Felipe, 46013 Valencia, Spain, and ^{||}Department of Bioregulation and Metabolism, Tokyo Metropolitan Institute of Medical Science, Tokyo 113-8613, Japan, Department of Physiology and Cell Biology, Tokyo Medical and Dental University, Tokyo 113-8519, Japan, and SORST, Japan Science and Technology Agency, Kawaguchi 332-0012, Japan

Atg4C/autophagin-3 is a member of a family of cysteine proteinases proposed to be involved in the processing and delipidation of the mammalian orthologues of yeast Atg8, an essential component of an ubiquitin-like modification system required for execution of autophagy. To date, the *in vivo* role of the different members of this family of proteinases remains unclear. To gain further insights into the functional relevance of Atg4C orthologues, we have generated mutant mice deficient in Atg4C/autophagin-3. These mice are viable and fertile and do not display any obvious abnormalities, indicating that they are able to develop the autophagic response required during the early neonatal period. However, *Atg4C*^{-/-}-starved mice show a decreased autophagic activity in the diaphragm as assessed by immunoblotting studies and by fluorescence microscopic analysis of samples from *Atg4C*^{-/-} GFP-LC3 transgenic mice. In addition, animals deficient in *Atg4C* show an increased susceptibility to develop fibrosarcomas induced by chemical carcinogens. Based on these results, we propose that *Atg4C* is not essential for autophagy development under normal conditions but is required for a proper autophagic response under stressful conditions such as prolonged starvation. We also propose that this enzyme could play an *in vivo* role in events associated with tumor progression.

The mechanisms responsible for delivering cytoplasmic cargo to the lysosome are known collectively as autophagy and play an important role in the maintenance of cell homeostasis (1–4). This process has been observed in all eukaryotic cells, indicating the widespread occurrence of this evolutionarily conserved pathway. Autophagy can be classified into at least three different pathways; that is, macroautophagy, microautophagy, and chaperone-mediated autophagy (4, 5). Macroautophagy is the major lysosomal route for the turnover of cytoplasmic components and will hereafter be referred as autophagy. This process begins with a sequestration event consisting of an

engulfment of cytoplasmic constituents by a membrane sac, called the isolation membrane. This structure results in a double-membrane vesicle called the autophagosome, containing bulk portions of cytoplasm, which eventually fuses with the lysosome. Finally, the inner membrane of the autophagosome and its protein and organelle contents are degraded by lysosomal hydrolases and recycled.

The knowledge of the molecular mechanisms underlying autophagy has considerably improved after the isolation and characterization of autophagy-defective mutants in the yeast *Saccharomyces cerevisiae* (6–9). A series of elegant studies directed to the functional characterization of these autophagy mutants has revealed that two ubiquitin-like conjugation systems are required for yeast autophagy (10, 11). One of these two systems requires the participation of Atg8 synthesized as a precursor protein, which is cleaved after a Gly residue by a cysteine proteinase called Atg4 (12–14). This Gly terminal residue from the modifier Atg8 is also activated by Atg7 (an ubiquitin-activating enzyme (E1)-like enzyme), but then the modifier protein is transferred to Atg3 (an ubiquitin carrier protein (E2)-like enzyme) and finally conjugated with membrane-bound phosphatidylethanolamine through an amide bond (11). The complex Atg8-phosphatidylethanolamine is also deconjugated by the proteinase Atg4, leading to the release of Atg8 from membranes. This modification system is an essential component of the membrane rearrangement dynamics taking place during the formation of autophagosomes and execution of autophagy. Several studies have shown that these ubiquitin-like conjugation systems associated with autophagy are conserved in higher eukaryotes (10, 15–18). Thus, proteins structurally and functionally related to the diverse yeast Atg proteins have been described in mammalian cells, and their roles in the process of autophagy have been elucidated in some cases (15, 16, 19). Recently we have described and cloned the four human orthologues of the yeast proteinase Atg4 (20). These proteins are members of the C-54 family of cysteine proteinases and maintain a significant sequence similarity with yeast Atg4. Human Atg4 orthologues also exhibit the structural features characteristic of the yeast proteinase including the catalytic Cys residue and its surrounding amino acid sequences. All of these structural features are also absolutely conserved in the amino acid sequence of the four murine orthologues of Atg4 (20).

* This work was supported by grants from Comisión Interministerial de Ciencia y Tecnología, Spain, Fundación Lilly, Fundación M. Botín, and European Union (Cancer Degradome-FP6). The costs of publication of this article were defrayed in part by the payment of page charges. This article must therefore be hereby marked "advertisement" in accordance with 18 U.S.C. Section 1734 solely to indicate this fact.

¹ Tel.: 34-985-104201; Fax: 34-985-103564; E-mail: clo@uniovi.es.

Autophagy Alterations and Increased Tumorigenesis in *Atg4C*^{-/-} Mice

The finding that the above-mentioned ubiquitin-like system is composed of four proteinases that may target at least six distinct substrates in mammals (LC3A, LC3B, LC3C, GATE-16, GABARAP, and ATG8L) (16, 21, 22) contrasts with the simplified yeast system involving a single proteinase with a specific substrate and indicates that this conjugation system has evolved to acquire a larger complexity during eukaryote evolution. Several works have shed some light on the involvement of Atg4 orthologues in the C-terminal processing and phosphatidylethanolamine deconjugation of some of the Atg8 mammalian orthologues (22–24). However, to date the *in vivo* role of the different members of this family of cysteine proteinases remains to be characterized. Similarly, it is unclear if the complexity of mammalian Atg4 orthologues and their putative substrates simply derives from functional redundancy in this system, as described for other protease families (25, 26), or by contrast it corresponds to a different scenario in which some components of this proteolytic system have evolved to accomplish other functions distinct from autophagy.

Among the four mammalian Atg4 orthologues, Atg4C is the most widely distributed in human tissues (20). On this basis together with the fact that human Atg4C is able to complement the deficiency of Atg4 in yeast, studies were undertaken to generate a murine model defective for the *Atg4C* gene. In this work we report the generation and phenotype analysis of mutant mice deficient in this member of the Atg4 family of cysteine proteinases. We show that these mice exhibit a tissue-specific decrease in autophagy in response to starvation, the main autophagy-inducing stimulus *in vivo*. In addition, *Atg4C*^{-/-} mice also show a decreased locomotor activity after prolonged starvation that could be correlated with their tissue-specific decrease in autophagic activity. Finally, we describe studies of cancer susceptibility in these mutant mice with the finding that *Atg4C* deficiency leads to an increased susceptibility to develop fibrosarcomas induced by chemical carcinogens. Based on these results, we conclude that the activity of this enzyme is not essential for a proper autophagic activity under normal circumstances but is required for an appropriate resistance to prolonged starvation *in vivo*. Finally, we propose that *Atg4C* could be involved in events associated with tumor progression.

EXPERIMENTAL PROCEDURES

Targeting Vector Construction—A genomic DNA clone was isolated from a mouse 129-SV/J genomic DNA library (Stratagene, La Jolla, CA), using a murine *Atg4C* cDNA fragment as probe. The genomic organization was determined by restriction analysis and subsequent subcloning of these fragments into pBluescript or pUC18. Plasmid pPN2T-Hgterm (kindly provided by Dr. C. Paszty, Lawrence Berkeley National Laboratory, Berkeley, CA) containing the *pgk-neo* and two *pgk-thk* (thymidine kinase) selection markers, was used to construct the *Atg4C* targeting vector. A 3.4-kb HindIII-BamHI fragment from the 5'-flanking region was used as the 5'-homologous region, whereas a 4.7-kb EcoRI-HincII fragment containing exons 5 and 6 was used as the 3'-region of homology. The 2.4-kb *neo* cassette was used as a positive marker and replaced a 10-kb fragment containing exons 1–4 of the *Atg4C* gene (Fig. 1A).

Generation of *Atg4C*-deficient Mice—The targeting vector was linearized by digestion with NotI, electroporated into HM1 embryonic stem cells, and selected for homologous recombination with G418 and ganciclovir. Positive clones were screened by Southern blot after PstI digestion of genomic DNA and probed with a radiolabeled 5'-external probe (Fig. 1B). A 12-kb fragment was detected from the wild-type allele, and an 8-kb fragment was detected from the corresponding mutant allele. The targeted embryonic stem cell clones were expanded and subsequently injected into blastocysts to generate chimeras. Chimeric males were mated with C57BL/6 female mice, and the offspring heterozygous for *Atg4C* were used to generate homozygous null mice. In all experiments homozygous *Atg4C*^{-/-} mice and their corresponding wild-type mice were littermates derived from interbreeding of heterozygotes with a mixed background of C57BL/6/129Sv. In all cases mice genotypes were determined by Southern blot analysis of tail DNA.

RT-PCR²—Total RNA was isolated from mouse tissues according to the method of Chomczynski and Sacchi (27). About half of the obtained product was reverse-transcribed using the RNA-PCR Core kit[®] from PerkinElmer Life Sciences. A PCR reaction was then performed with mouse *Atg4C*-specific primers for 25 cycles of denaturation (94 °C, 20 s), annealing (62 °C, 20 s), and extension (72 °C, 30 s). As a control, β -actin was PCR-amplified from all samples under the same conditions.

Immunoblotting—Mice tissues were immediately frozen in liquid nitrogen after extraction and were homogenized in a 20 mM Tris buffer, pH 7.4, containing 150 mM NaCl, 1% Triton X-100, 10 mM EDTA, and Complete[®] protease inhibitor mixture (Roche Applied Science). Once homogenized, tissue extracts were centrifuged at 12,000 rpm at 4 °C, and supernatants were collected. The protein concentration of the supernatant was evaluated by bicinchoninic acid technique (BCA protein assay kit, Pierce). 25 μ g of protein sample was loaded on 13% SDS-polyacrylamide gels. After electrophoresis, gels were electrotransferred onto nitrocellulose filters, and then the filters were blocked with 5% nonfat dried milk in PBT (phosphate-buffered saline with 0.05% Tween 20) and incubated with primary antibodies in 5% bovine serum albumin in PBT. After three washes with PBT, filters were incubated with horseradish peroxidase-conjugated goat anti-rabbit IgG at a 1:10,000 dilution in 1.5% milk in PBT and developed with a West Pico enhanced chemiluminescence kit (Pierce). The antibodies against Atg4C, GATE-16, GABARAP, and LC3 were kindly provided by Dr. T. Ueno (Juntendo University, Tokyo). The antibodies against Atg4A, Atg4B, and Atg4D were from Abgene (Manchester, UK).

Northern Blot Analysis—Nylon filters containing 2 μ g of poly(A)⁺ RNA of a wide variety of murine tissues were prehybridized at 42 °C for 3 h in 50% formamide, 5 \times saline/sodium phosphate/EDTA (1 \times saline/sodium phosphate/EDTA, 150 mM NaCl, 10 mM NaH₂PO₄, 1 mM EDTA, pH 7.4), 10 \times Denhardt's solution, 2% SDS, and 100 μ g/ml denatured herring

² The abbreviations used are: RT, reverse transcription; GFP, green fluorescent protein; MCA, methylcholanthrene; PBS, phosphate-buffered saline; DMEM, Dulbecco's modified Eagle's medium; GABARAP, γ -aminobutyric acid receptor-associated protein.

sperm DNA. Filters were then hybridized with radiolabeled probes for each full-length clone cDNA. Hybridization was performed for 20 h (under the same conditions. Filters were washed with 0.1× SSC ((1× SSC = 0.15 M NaCl and 0.015 M sodium

citrate)) and 0.1% SDS for 2 h at 50 °C, and exposed to autoradiography. RNA integrity and equal loading were assessed by hybridization with an actin probe.

Quantitative Real-time PCR—Total RNA was extracted

from mouse tissues using the RNeasy kit (Qiagen, Valencia, CA) according to the manufacturer's protocol. cDNA was synthesized using 1–5 μg of total RNA, 0.14 mM oligo(dT) (22-mer) primer, 0.2 mM concentrations of each deoxynucleoside triphosphate, and Superscript II reverse transcriptase (Invitrogen). Quantitative reverse transcription-PCR was carried out in triplicate for each sample using 20 ng of cDNA, TaqMan® Universal PCR master mix (Applied Biosystems, San Francisco, CA), and 1 μl of the specific TaqMan® custom gene expression assay for *Atg4A*, *Atg4B*, *Atg4C*, and *Atg4D* (Applied Biosystems). To quantitate gene expression, PCR was performed at 95 °C for 10 min followed by 40 cycles of 95 °C for 15 s, 60 °C for 30 s, and 72 °C for 30 s using an ABI Prism 7700 sequence detector system. As an internal control for the amount of template cDNA used,

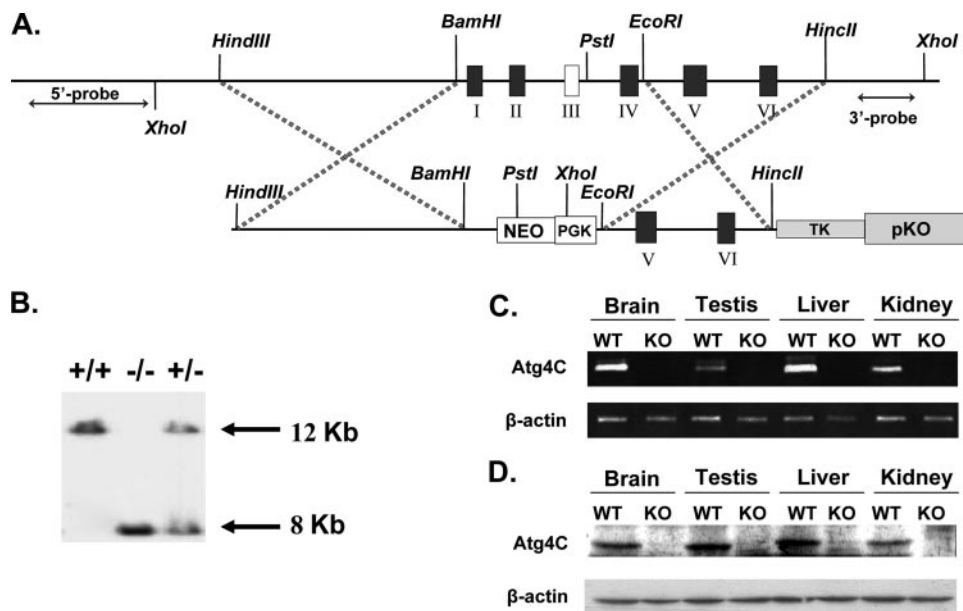


FIGURE 1. Targeted disruption of the *Atg4C* gene. *A*, upper, genomic organization of the *Atg4C* locus. Lower, the targeting construct replaces exons I–IV, including the catalytic domain of *Atg4C* (exon III), with the neomycin gene driven by the 3-phosphoglycerate kinase promoter. *B*, Southern blot of DNA from wild-type, heterozygous, and knock-out mice tails. Hybridization with the 3'-external probe detects 12- and 8-kb *PstI* bands representing wild-type and mutant alleles, respectively. *C*, RT-PCR of RNA of diverse tissues from wild-type (WT) and *Atg4C*^{-/-} (KO) mice showing the absence of full-length *Atg4C* mRNA expression in mutant mice. *D*, immunoblotting of protein extracts of diverse tissues from wild-type and *Atg4C* knock-out mice.

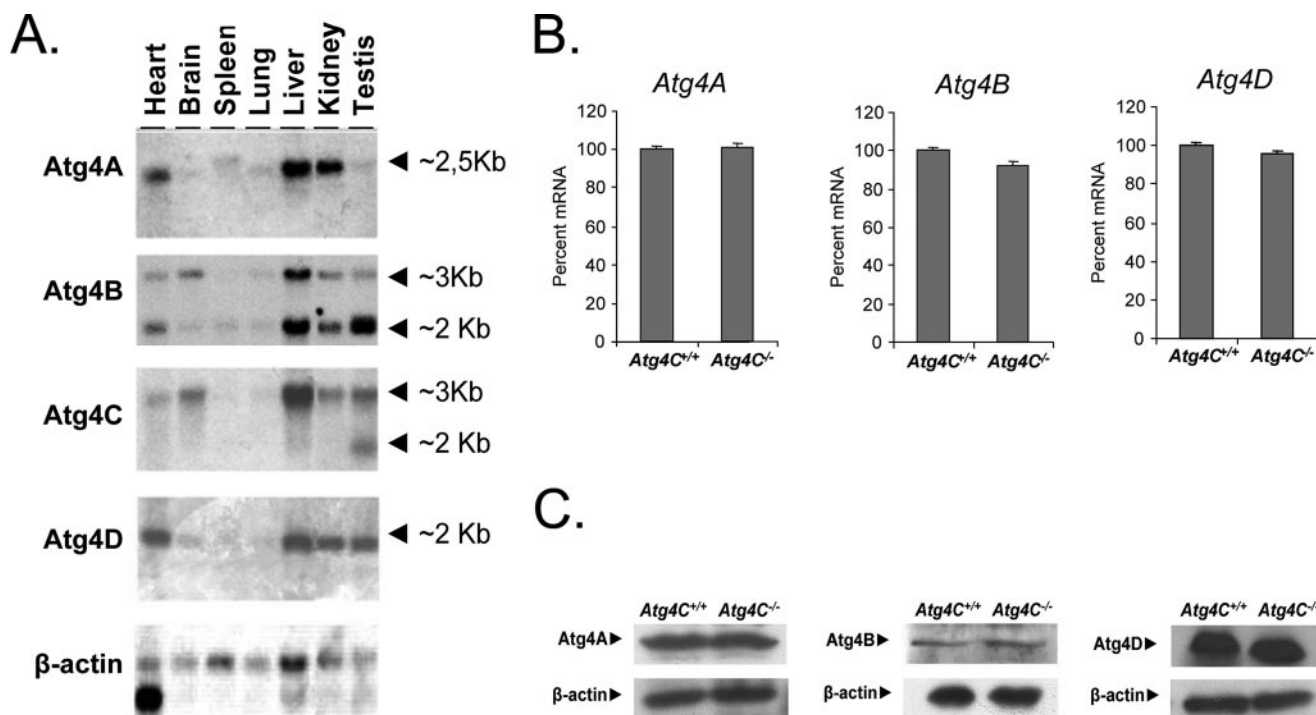
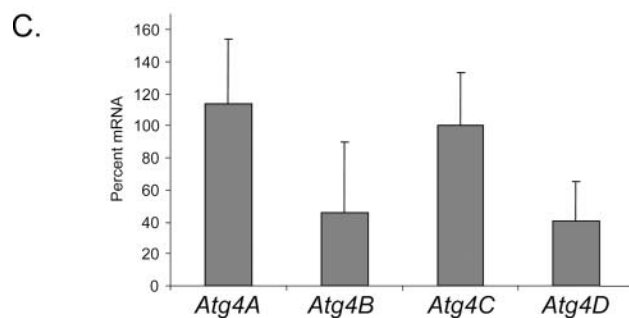
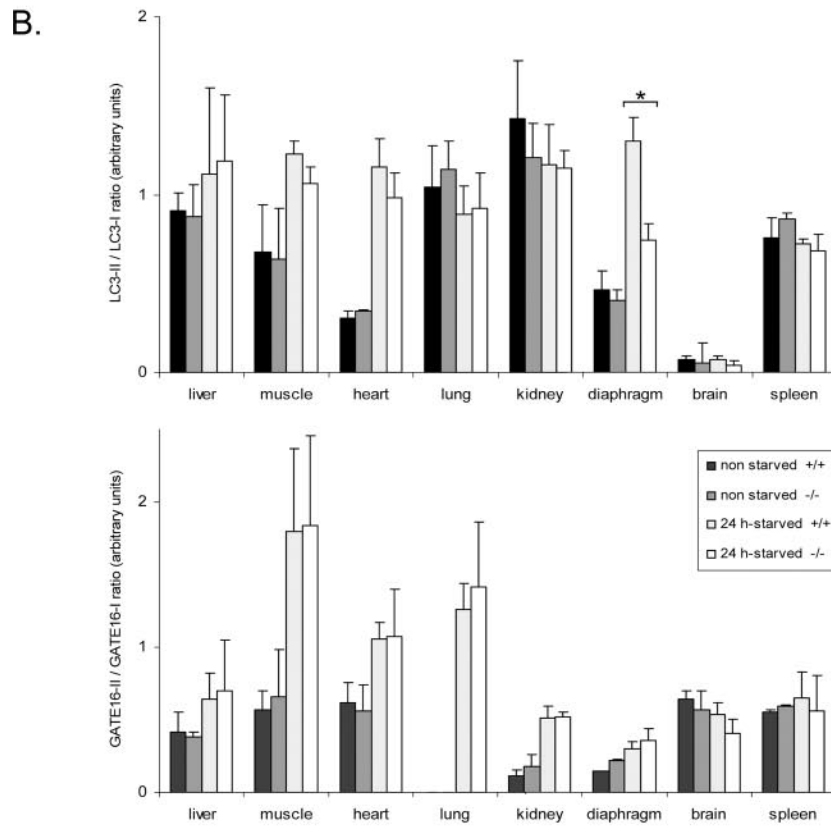
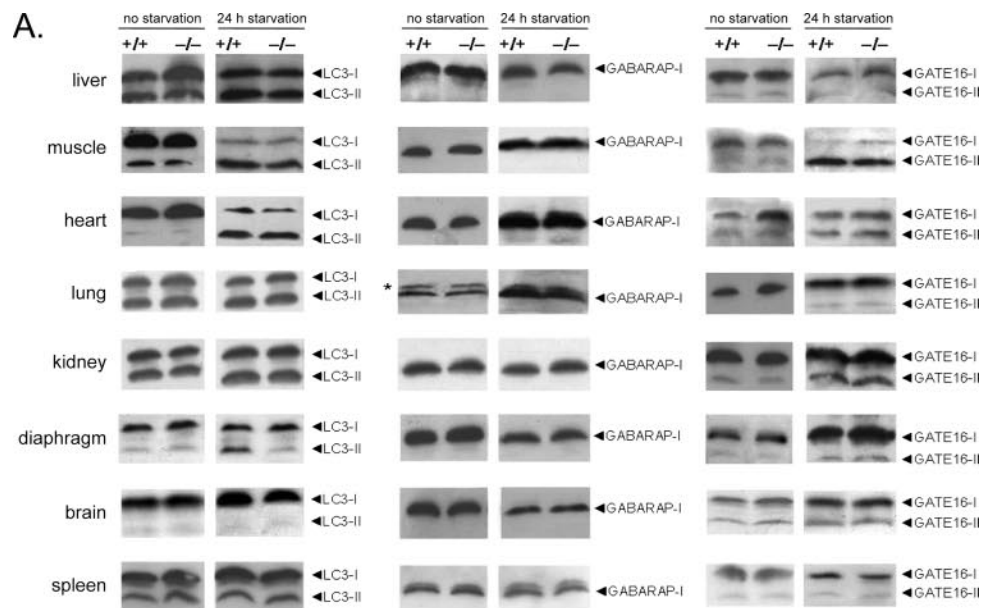


FIGURE 2. Expression and immunoblotting analysis of *Atg4* orthologues in murine tissues. *A*, filters containing ~2 μg of polyadenylated RNAs from the indicated murine tissues were hybridized with specific probes for mouse *Atg4* orthologues. Approximate RNA sizes are indicated. Filters were subsequently hybridized with a murine actin probe to ascertain the differences in RNA loading among the different samples. *B*, expression analysis of *Atg4a*, *Atg4b*, and *Atg4d* in livers from starved wild-type and *Atg4C*^{-/-} mice. The transcript expression levels are relative to that in the wild-type, which was set at 100%. *C*, immunoblotting using antibodies against *Atg4A*, *Atg4B*, and *Atg4D* in total protein extracts of skin from wild-type and *Atg4C* knock-out mice.

Autophagy Alterations and Increased Tumorigenesis in *Atg4C*^{-/-} Mice



gene expression was normalized to the mouse glyceraldehyde-3-phosphate dehydrogenase (GAPDH) gene using the Mouse GAPD (GAPDH) Endogenous Control (VIC[®]/MGB Probe, Primer Ltd) TaqMan[®] Gene expression assay (Applied Biosystems). Relative expression of the distinct *Atg4* genes was calculated according to manufacturer's instructions. Briefly, *Atg4A*, *Atg4B*, *Atg4C*, and *Atg4D* expression was normalized to glyceraldehyde-3-phosphate dehydrogenase in wild-type or *Atg4C*^{-/-} derived samples using the following formula: the mean values of $2^{\Delta\Delta CT_{\text{gene}}(\text{Atg4A, Atg4B, Atg4C, or Atg4D}) - \Delta CT_{\text{gene}}(\text{GAPDH})}$ for three different wild-type animals were considered 100% for each *Atg4* gene, and the same values for *Atg4C*^{-/-} mice tissues were referred to those values according to Livak and Schmittgen (28).

Quantitative Analysis of GFP-LC3 Dots—Mutant mice deficient in *Atg4C* were crossed with transgenic mice overexpressing GFP-LC3 that provide an efficient *in vivo* marker for autophagy (29). To avoid autophagy induction, mice were perfused with 4% paraformaldehyde in 0.1 M sodium phosphate buffer (PBS), pH 7.4. Tissues were harvested and further fixed with the same fixative solution for at least 4 h followed by treatment with 15% sucrose in PBS for 4 h, and then with 30% sucrose solution overnight. Tissue samples were embedded in Tissue-Tek OCT compound (Sakura Finetechnical Co. Ltd., Tokyo, Japan) and stored at -70 °C. Samples were then sectioned at 5- μ m of thickness with cryostat (CM3050 S, Leica, Deerfield, IL), air-dried for 1 h, washed in PBS for 5 min, dried at room temperature for 30 min, and mounted with conventional anti-fading medium. The number of GFP-LC3 dots was counted in five independent visual fields from at least five independent mice in each organ using a Leica TCS sp2 AOBs confocal fluorescence microscope.

Measurement of Locomotor Activity of Mice—To monitor the locomotor activity of mice, an actimeter (LE 8811 Motor activity Monitor, Leticia, Spain) was used. Animals were placed alone in plastic cages inside the actimeter, and cages were washed between measurements to avoid possible alterations in mice behavior. The movements of each animal were recorded during 10 min.

Carcinogenesis Protocols and Analysis of Tumors—Mouse experimentation was done in accordance with the guidelines of the Universidad de Oviedo (Spain), regarding the care and use of laboratory animals. For methylcholanthrene (MCA) chemical carcinogenesis, groups of mice were injected subcutaneously with a freshly prepared solution of MCA in olive oil (100 mg in 100 ml per mouse). Mice were weekly monitored for tumor development over the course of 8–20 weeks. Tumors larger than 5 mm and showing progressive growth were counted as positive and confirmed thereafter by histological

analysis. Mice were sacrificed when they had an overt tumor mass or they looked moribund. After conventional staining with hematoxylin and eosin, cells were morphologically identified by an expert pathologist and counted with no previous knowledge of mice phenotypes.

Fibroblast Extraction and Culture—Adult murine fibroblasts were extracted from 12-week-old mice ears. Ears were sterilized with ethanol, washed with PBS, and triturated with razor blades. Samples were then incubated with 600 ml of 4 mg/ml collagenase D (Roche Applied Science) and 4 mg/ml dispase II (Roche Applied Science) in Dulbecco's modified Eagle's medium (DMEM; Invitrogen) for 45 min at 37 °C and 5% CO₂. After filtering and washing, 6 ml of DMEM with 10% fetal bovine serum (Invitrogen), and 1% antimycotic-antibiotic (Invitrogen) were added, and the mixture was incubated at 37 °C and 5% CO₂. Once extracted, cells were cultured in DMEM containing 10% fetal bovine serum at 37 °C and 5% CO₂.

Protein Degradation Assays—To label proteins, adult murine fibroblasts were incubated at 37 °C for 48 h in complete fresh DMEM (Sigma) containing 10% (v/v) fetal bovine serum (Invitrogen), 1% antimycotic-antibiotic (Invitrogen) and with 5 μ Ci/ml L-[³H]leucine (Amersham Biosciences). Before the proteolysis experiments were started, cells were washed once with PBS containing 2 mM L-leucine and chased at 37 °C for 24 h in complete DMEM containing 10% (v/v) fetal bovine serum, 1% antimycotic-antibiotic, and 2 mM L-leucine to eliminate short-lived proteins. Proteolysis experiments and measurements of intracellular protein degradation were carried out as described previously (30) using 3-methyladenine to specifically inhibit autophagic degradation. Protein degradation was analyzed 1 h after the addition of the 3-methyladenine and for an additional period of only 3 h to ensure optimal inhibition and to avoid possible secondary effects of the inhibitor. All experiments were performed at least four times with duplicate samples and using independent cell lines.

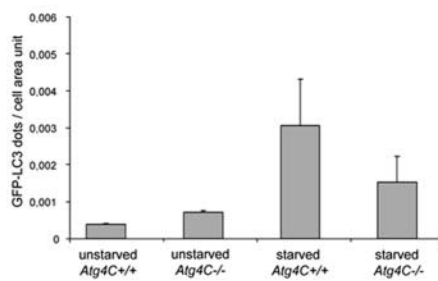
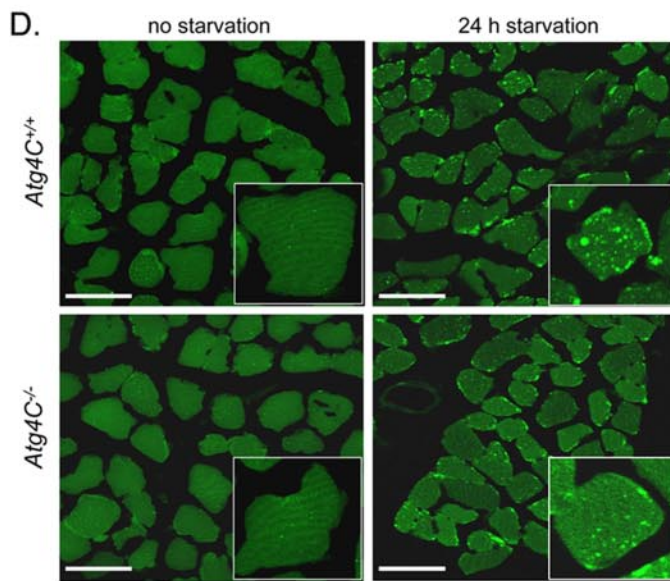
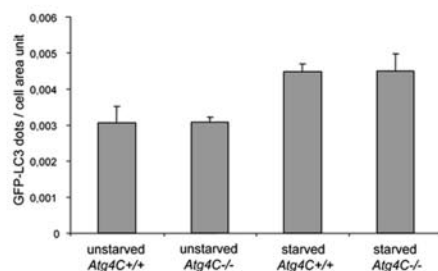
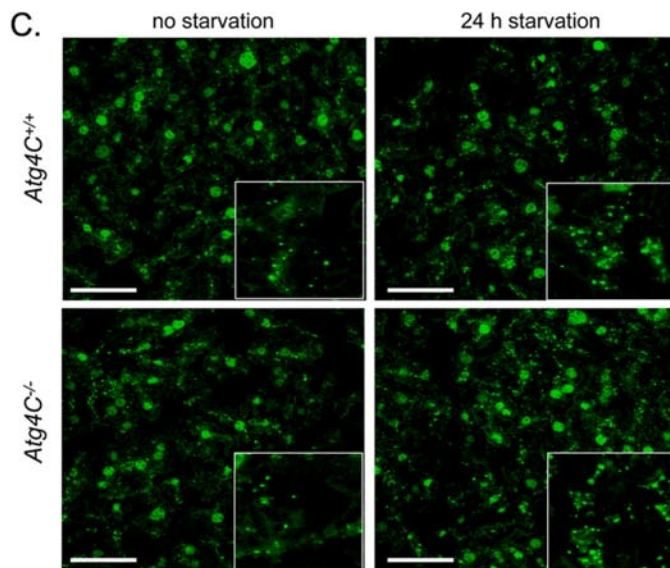
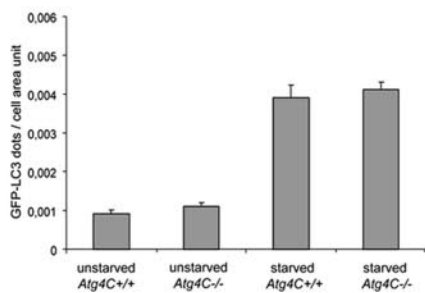
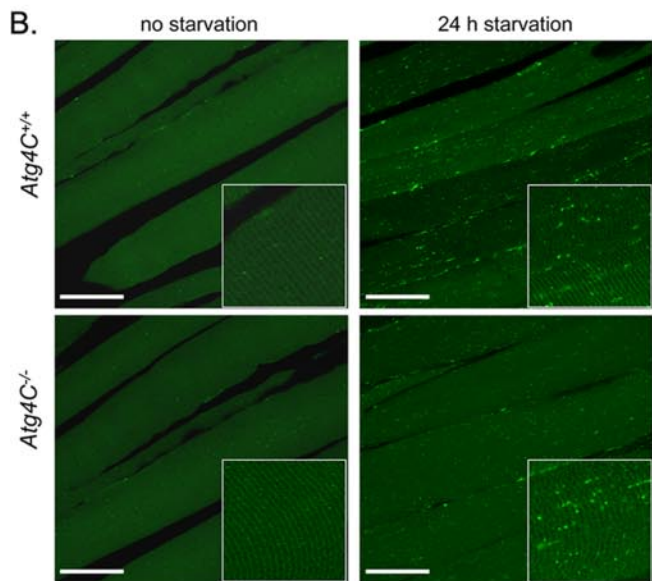
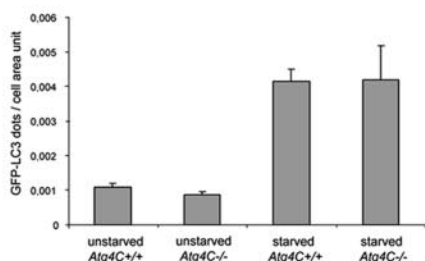
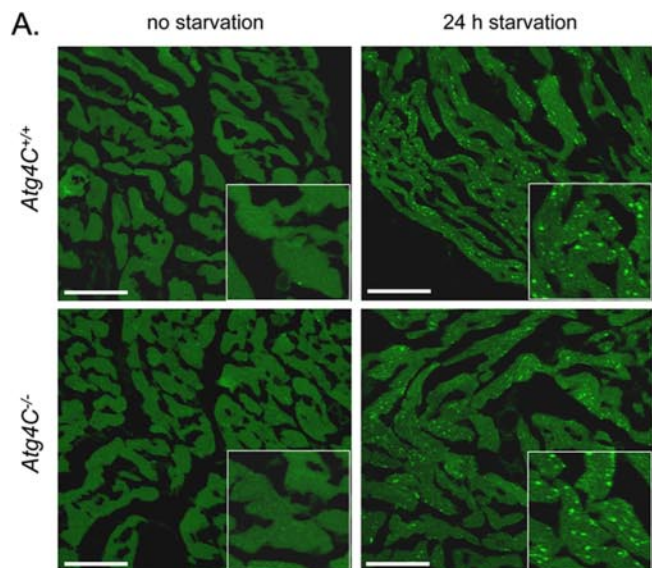
Statistical Analysis—All experimental data are reported as the mean, and the error bars represent the experimental S.E. Statistical analysis were performed by the non-parametric Student's *t* test excepting for MCA-tumor induction statistical analysis, which was evaluated using the Kaplan-Meier method (31) and compared with the log-rank test. Statistical analyses were made using the Prism program Version 4.0 (GraphPad Software, Inc).

RESULTS

Generation of *Atg4C*-deficient Mice—To examine the *in vivo* function of *Atg4C*, we generated mice with a targeted mutation in the *Atg4C* gene. A genomic clone encoding *Atg4C* was obtained from a mouse 129-SV/J genomic DNA library and

FIGURE 3. Analysis of LC3, GATE-16, and GABARAP status in *Atg4C*^{-/-} mice. *A*, wild-type and *Atg4C*^{-/-} mice of 12 weeks of age were fed *ad libitum* or starved for 24 h and then sacrificed. A variety of tissues from these mice were extracted and homogenized as described under "Experimental Procedures." Panels show representative immunoblots against LC3, GATE-16, and GABARAP in multiple tissues from wild-type and *Atg4C*^{-/-} mice. LC3-I (~19 kDa), GATE-16-I (~17 kDa), and GABARAP-I (~16 kDa) stand for the cytosolic forms of these proteins, whereas LC3-II (~16 kDa) and GATE-16-II (~15 kDa) stand for the lipidated forms of these proteins. The asterisk stands for a nonspecific band. *B*, densitometry analysis of the immunoblots against LC3 and GATE-16 in tissues from *Atg4C*^{+/+} and *Atg4C*^{-/-} mice. Bars represent the lipidation status of GATE-16 and LC3. At least four *Atg4C*^{-/-} and 4 *Atg4C*^{+/+} mice were used for this experiment. In the case of heart and diaphragm tissues, 12 *Atg4C*^{-/-} and 12 *Atg4C*^{+/+} mice were used. The asterisk indicates differences found to be statistically significant at *p* < 0.05. *C*, expression analysis of *Atg4A*, *Atg4B*, *Atg4C*, and *Atg4D* in diaphragms from wild-type and *Atg4C*^{-/-} mice. The transcript expression levels are relative to *Atg4C* expression level, which was set at 100%.

Autophagy Alterations and Increased Tumorigenesis in *Atg4C*^{-/-} Mice



used for construction of the targeting vector (Fig. 1A). This vector was designed to allow the replacement of exons 1, 2, 3, and 4 of the endogenous *Atg4C* gene with a *neo* cassette (Fig. 1A). The linearized targeting vector was electroporated into HM-1 embryonic stem cells, and 4 clones that were positive for homologous recombination were used to generate chimeric founder mice. Heterozygous mice from the F1 generation were identified by Southern blot analysis and then crossed to obtain *Atg4C*^{-/-} mice (Fig. 1B). RT-PCR analysis of total RNA from diverse tissues of wild-type and knock-out animals revealed that the *Atg4C* transcript was absent in *Atg4C*^{-/-} mice (Fig. 1C). The same negative results were obtained by immunoblotting of these tissues (Fig. 1D), confirming the generation of an *Atg4C*-null allele.

Normal Development and Growth of *Atg4C*^{-/-} Mice—Despite the *Atg4C* deficiency, mutant mice developed normally with males and females being fertile. Likewise, there were no gross detectable differences between the growth curves of wild-type and knock-out mice. In addition, the mutant mice showed no overt phenotype, and their long-term survival rates were indistinguishable from those of their wild-type littermates. Histopathological analysis of diverse tissues from adult *Atg4C*^{-/-} animals revealed no observable differences with wild-type tissues (data not shown). Similarly, plasma levels of amino acids and major biochemical parameters (including glucose, cholesterol, triglycerides, uric acid, creatine kinase, aldosterone, and hepatic aminotransferases) were similar to the levels of their wild-type littermates. Taken together, these data demonstrate that *Atg4C* is dispensable for embryonic and adult mouse development as well as for normal growth and fertility.

The above findings showing that the development of mice deficient for *Atg4C* is normal suggest that this protein is not necessary for the induction of the requested level of autophagy which has been proved to be essential for the viability of neonate mice (32, 33). A functional redundancy in the *Atg4* family of cysteine proteinases, which has been previously reported for other protease families (25, 26, 34–36), could contribute to explain this observation. To test this possibility, we examined by Northern blot analysis the expression profile of these genes in a variety of mouse tissues including testis, spleen, kidney, skeletal muscle, liver, lung, brain, and heart (Fig. 2A). We observed that the expression pattern of the four *Atg4* genes is very similar in murine tissues. This could explain at least in part the fact that the activity of *Atg4C* is not essential to generate the sufficient basal autophagy requested under normal circumstances in any of the tissues analyzed. Given this overlapping expression pattern in the *Atg4* gene family, we examined whether the loss of *Atg4C* activity *in vivo* could modulate the levels of other *Atg4* cysteine proteinases. To test this hypothesis, we first analyzed by quantitative RT-PCR the *Atg4A*, *Atg4B*, and *Atg4D* transcript levels in the livers of 48-h-starved *Atg4C*^{-/-} and *Atg4C*^{+/+} mice. As shown in Fig. 2B, a consist-

ent change in the relative expression levels of *Atg4* genes was not detected. We next analyzed the protein levels of *Atg4A*, *Atg4B*, and *Atg4D* in *Atg4C*^{-/-} and *Atg4C*^{+/+} tissues. As shown in Fig. 2C and in agreement with our quantitative PCR results, we did not observe any significant change in the protein levels of the different *Atg4* enzymes in *Atg4C*^{-/-} tissues. Finally, to evaluate a possible change in the subcellular distribution of these proteins in the absence of *Atg4C*, we analyzed the localization of the other *Atg4* family members in *Atg4C*^{-/-} cells, but we did not find any evidence supporting putative changes in the distribution of these proteins (data not shown). Taken together, these results do not provide evidence for a compensatory mechanism in *Atg4C*-deficient mice.

Atg4C* Gene Disruption Leads to a Tissue-specific Decrease of Autophagy *in Vivo—The fact that *Atg4C*^{-/-} mice develop normally suggests that autophagy is not impaired in the absence of *Atg4C*. However, it should be emphasized that previous studies with other mutant mice exhibiting reduced autophagic activity have demonstrated that a decrease in this process is not necessarily accompanied by perinatal lethality (37, 38).

To test the possibility that *Atg4C* disruption leads to a decrease in autophagy but not to its total impairment, we performed immunoblotting studies in tissue extracts from mutant and control mice fed *ad libitum* or after 24 h of starvation, which has been shown to be the main stimulus for *in vivo* induction of autophagy (29). We focused on the analysis of the molecular forms of LC3B (referred hereafter as LC3), GATE-16, and GABARAP. These proteins are the major mammalian orthologues of yeast *Atg8* detected in autophagosome membranes (39). As shown in Fig. 3, we were able to detect the lipidated forms of LC3 and GATE-16 in *Atg4C*^{-/-} mice in the same tissues as in wild-type animals, whereas we could not detect the lipidated form of GABARAP either in wild-type nor in *Atg4C*^{-/-} mice, demonstrating that *Atg4C* activity is not essential for the processing of these proteins *in vivo*. However, we observed that the ratio of LC3-II/LC3-I, which has been widely used as an indicator of autophagic activity, was significantly decreased in the diaphragm muscle of starved *Atg4C*^{-/-} mice (Fig. 3B). We also analyzed by quantitative RT-PCR the relative expression level of the distinct *Atg4* cysteine proteinases in the diaphragm with the finding of a high relative expression of *Atg4C* in this tissue (Fig. 3C).

To confirm and extend these observations pointing to a tissue-specific reduction of autophagic responses in *Atg4C*^{-/-} mice, we crossed these mutant mice with those expressing the transgene GFP-LC3 that provides an efficient *in vivo* marker for autophagy (29, 37, 40, 41). Fluorescence microscopic analysis of diverse tissues revealed that the number of punctate GFP-LC3 structures is equivalent in tissues from non-starved wild-type or *Atg4C*^{-/-} mice (Fig. 4). Similarly, we were not able to detect any significant change in the number of GFP-LC3 punctate structures in the majority of tissues analyzed after 24 or 48 h of

FIGURE 4. Fluorescence analysis of tissues from wild-type and *Atg4C*^{-/-} GFP-LC3 expressing mice fed *ad libitum* or after 24 h of starvation. Representative images and quantitation of GFP-LC3-positive dots in cryosections of different tissues from 2-month-old wild-type and *Atg4C*^{-/-} mice stably expressing the GFP-LC3 transgene (A, heart. B, skeletal muscle. C, liver. D, diaphragm). The number of GFP-LC3 dots was counted and divided by the corresponding area. The x axis labels denote *Atg4C* genotype. Results shown represent the mean of 10 images from every tissue per mice obtained from 5 mice per genotype. Note that the nuclei of liver cells shows nonspecific green fluorescence in C.

Autophagy Alterations and Increased Tumorigenesis in *Atg4C*^{-/-} Mice

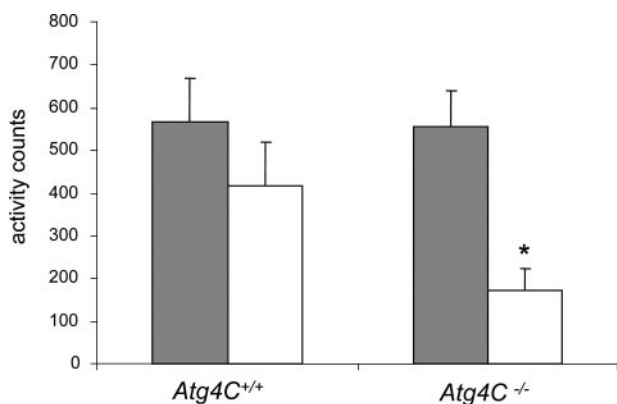


FIGURE 5. Locomotor activity analysis of *Atg4C*^{-/-} and wild-type mice after prolonged starvation. Mice were placed in a plastic cage inside a photocell actimeter for 10 min in silence to monitor their locomotor activity. Plastic cages were washed between measurements to avoid possible alterations in mice behavior. The activity counts registered by actimeter represent the number of longitudinal movements of mice during the time of the analysis. 15 *Atg4C*^{-/-} and 15 wild-type mice were used in this experiment for each condition. The locomotor activity of animals fed *ad libitum* is represented by gray bars, whereas white bars represent the locomotor activity of 48 h-starved mice. The asterisk indicates differences found to be statistically significant at $p < 0.05$.

starvation (Fig. 4 and data not shown). However, in agreement with our immunoblotting results, we could detect a clear decrease in the number of GFP-LC3 punctate structures per cell area unit in the diaphragms from 24-h-starved *Atg4C*^{-/-} mice as compared with their wild-type littermates (Fig. 4D). Although not statistically significant, the analysis of GFP-LC3 distribution in the diaphragm reveals a clear trend toward a reduction of autophagic activity in the diaphragm of starved *Atg4C*^{-/-} mice as compared with wild-type animals, thus confirming and extending the above immunoblotting results.

***Atg4C* Gene Disruption Leads to Reduced Locomotor Activity in Response to Starvation**—In the course of the different starvation treatments performed to induce autophagy, we could observe a reduced resistance to prolonged starvation in mice deficient in *Atg4C* as compared with wild-type animals. In fact, mutant mice showed a less healthy appearance and a reduced mobility than wild-type animals subjected to the same conditions, and some of them even succumbed to starvation after 48 h (data not shown). By contrast and as previously reported (29), wild-type animals were able to resist periods of 48 h of starvation. To further extend this observation, we performed an analysis of the locomotor activity of *Atg4C*^{-/-} mice and their wild-type littermates fed *ad libitum* or subjected to 48 h starvation using a photocell actimeter, an apparatus that allows the recording of the movements and crossings of mice (42, 43). As shown in Fig. 5, the locomotor activity of non-starved *Atg4C*^{-/-} mice was similar to control mice. However, after prolonged starvation, the locomotor activity of null mice was significantly reduced as compared with wild-type animals. Thus, it is tempting to speculate that the diminished capacity of inducing autophagy in diaphragm from *Atg4C*^{-/-} mice leads to a reduced resistance to starvation that results in a reduced mobility in these mutant animals. Nevertheless, we cannot rule out the possibility that additional factors could contribute to explain

the observed reduced resistance to starvation of *Atg4C*^{-/-} mice.

Increased Susceptibility of *Atg4C*-deficient Mice to MCA-induced Fibrosarcomas—Many works have analyzed the putative correlations between the ability of cancer cells for developing autophagy and their neoplastic potential (44–46). The fact that *beclin-1* haplo-deficient mice, which show a decrease in autophagy, also exhibit a high incidence of spontaneous tumors supports the idea that an autophagy decrease can confer an increased susceptibility to cancer (37, 38). On this basis and considering that *Atg4C*^{-/-} disruption leads to a decrease in autophagy under demanding conditions, we were prompted to test the hypothesis that the absence of this proteinase could be associated with an increase in cancer susceptibility in these mutant mice. Because our first studies to examine this possibility indicated that *Atg4C*^{-/-} mice do not develop more spontaneous tumors than their wild-type littermates (data not shown), we next focused on the comparative analysis of the susceptibility of these mice to cancer induced by chemical carcinogens. To this purpose, wild-type and *Atg4C* mutant mice were induced to develop fibrosarcomas using a carcinogenesis protocol based on the intradermal injection of a single dose of the carcinogen MCA, as previously described (47, 48). This chemical carcinogen promotes the transformation of mesenchymal fibroblasts into fibrosarcomas. As shown in Fig. 6A, fibrosarcomas arose more rapidly and with a significantly higher incidence in *Atg4C*^{-/-} mice than in wild-type animals. These differences in number of fibrosarcomas between mutant mice and wild-type controls were statistically significant. Histological analysis of fibrosarcomas generated in both wild-type and *Atg4C*^{-/-} male mice revealed that most of them (80%) were partially infiltrative grade I fibrosarcomas (with absence of necrosis, undifferentiated, and with 2 or 3 mitosis by each high magnification field), and only exceptionally gave rise to more aggressive grade II tumors (Fig. 6B). These results suggest that the absence of *Atg4C* does not influence the late stages of tumor development in male mice.

To test the possibility that a decrease in autophagy due to *Atg4C* disruption leads to the higher incidence of fibrosarcomas observed in mutant mice, we studied the autophagic activity of adult murine fibroblasts, cells in which *Atg4C* is highly expressed (Fig. 7A). For that purpose, we analyzed the *in vitro* degradation of long-lived proteins in fibroblasts derived from *Atg4C*^{-/-} mice and their wild-type littermates. As previously reported (30), we employed the autophagy inhibitor 3-methyladenine to measure the autophagy-mediated proteolysis in cultured cells. As expected, *Atg4C*^{-/-} fibroblasts did not show changes in protein degradation under confluent growing in normal conditions (Fig. 7B). However, under serum and amino acids deprivation, *Atg4C*^{-/-} cells showed a lower rate of 3-methyladenine sensitive protein degradation, which represented autophagic degradation, than the corresponding controls (Fig. 7C). To test if the observed reduction of autophagic degradation was due to the lack of *Atg4C* or to other causes, we transfected *Atg4C*^{-/-} cells with an eukaryotic expression vector con-

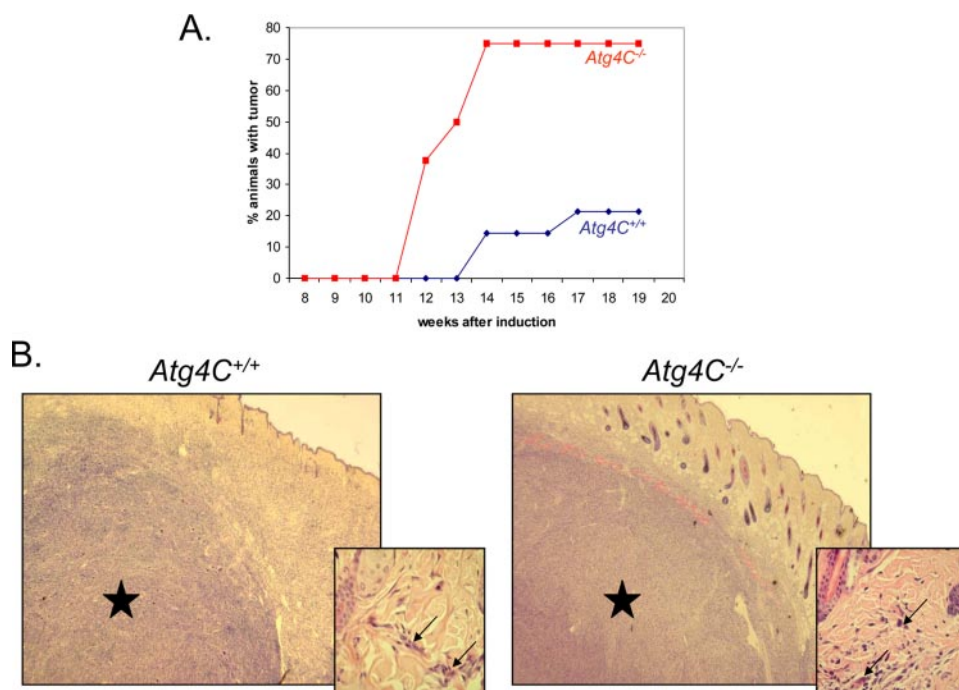


FIGURE 6. Induced tumorigenesis in *Atg4C*^{-/-} and wild-type mice. *A*, percentage of mice with tumor among *Atg4C*^{+/+} (◆) or *Atg4C*^{-/-} (■) male mice injected with 100 μ g of MCA; eight mice for each phenotype were used for this experiment. *B*, representative pictures taken from hematoxylin and eosin stained tissue sections from *Atg4C*^{+/+} or *Atg4C*^{-/-} tumors showing that there are no significant differences in the grade of invasiveness of tumors from both genotypes. Stars indicate fibrosarcomas partially infiltrating normal tissue, whereas arrows indicate tumor cells that migrate through normal skin tissue.

taining the *Atg4C* cDNA and measured the autophagic activity of transfected cells under starvation conditions. As shown in Fig. 7D, the autophagic degradation levels of *Atg4C*-transfected mutant cells were comparable with those obtained with control cells, indicating that the loss of *Atg4C* leads to a reduced autophagic degradation *in vitro* under starvation conditions. Taken together, these results support the idea of a reduced capacity of *Atg4C*^{-/-} cells to develop a proper autophagic response under compromising conditions. This fact could contribute to explaining the higher incidence of fibrosarcomas observed in null mice after chemical carcinogen induction.

DISCUSSION

To date, the precise *in vivo* role of the four members of the mammalian Atg4 family of cysteine proteinases remains to be characterized. So far, it is not known whether the existence of four mammalian orthologues of the yeast protease Atg4 corresponds to a functional redundancy or, by contrast, the components of this proteolytic system have acquired other functions distinct from autophagy during eukaryote evolution. As a first step to address this issue, we describe in this work the generation and phenotype analysis of mutant mice deficient in *Atg4C*, a member of the Atg4 family of cysteine proteinases that exhibits a wide tissue distribution and complements the deficiency of yeast Atg4 in autophagic processes. However, despite the wide expression pattern of *Atg4C* under normal conditions, targeted disruption of this gene in mice does not cause any major abnormalities. Thus, *Atg4C*^{-/-} mice develop normally, are fertile, and have long

term survival rates indistinguishable from those of wild-type mice. These observations suggest that *Atg4C* gene disruption does not impair the ability of cells to undergo a proper autophagic response after birth, which has been proven to be essential for neonate viability.

To evaluate the involvement of *Atg4C* in the processing and delipidation of Atg8 orthologues *in vivo*, we first performed immunoblot analysis of their putative major substrates LC3, GATE-16, and GABARAP. These studies revealed that the lipidated forms of LC3 and GATE-16 were present in the majority of the analyzed tissues from both mutant and wild-type animals at a similar extent, whereas we could not detect the lipidated form of GABARAP in any of the tissues analyzed. The absence of GABARAP lipidation even under strong starvation conditions provides support to the idea that the major physiological function of this protein is not related to autophagic

degradation (49, 50). All these observations suggest that *Atg4C* is not essential for the processing or delipidation of Atg8 orthologues. However, we found that under starvation conditions, the lipidation status of LC3 in the diaphragm, a continuous energy-consuming muscle, was diminished in mutant mice. This observation was confirmed by crossing *Atg4C*^{-/-} mice with transgenic mice overexpressing GFP-LC3. *Atg4C*^{-/-} mice showed a slight but significant decrease in the number of GFP-LC3 punctate structures, which was associated with a decrease in autophagy in diaphragm under starvation conditions.

The fact that *Atg4C* activity is not essential for the development of autophagy under normal conditions might be explained by a functional redundancy in the Atg4 family of cysteine proteinases, as previously reported for other proteinase families from different catalytic classes (25, 35, 36, 51). Our finding of a considerable overlapping in the tissue distribution of the different mouse Atg4 orthologues should be consistent with the proposal of a functional redundancy in the Atg4 family of proteinases. However, despite this apparent redundancy observed in the Atg4 family, the finding that autophagy is reduced after 24 h of starvation in diaphragm from *Atg4C*-deficient mice muscle suggests that only under very demanding conditions, *Atg4C* activity is necessary for a proper autophagic response. Likewise, the reduced locomotor activity observed in *Atg4C*^{-/-} mice after prolonged starvation could be a consequence of the decrease of autophagic activity in the diaphragm. Further works aimed to study metabolic and respiratory functions of

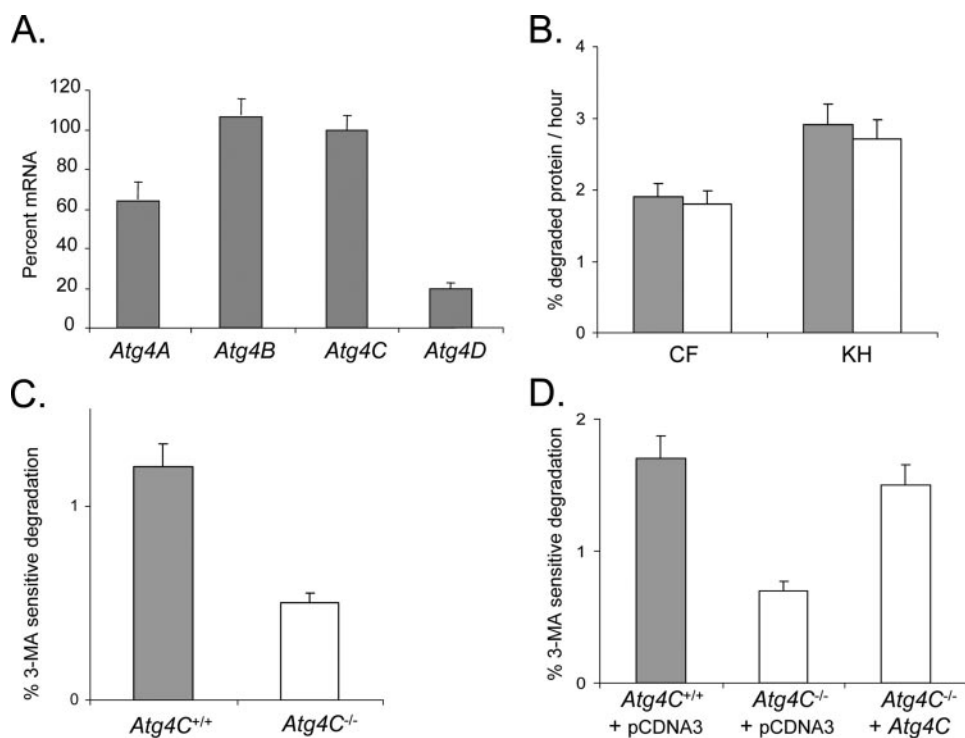


FIGURE 7. Analysis of the autophagic activity of *Atg4C*^{-/-} and wild-type adult murine fibroblasts. Fibroblasts were metabolically labeled and chased as described under "Experimental Procedures." Confluent cells were then switched to complete (CF) or serum- and amino acid-deficient (KH) media with or without 3-methyladenine. To allow optimal inhibition and to avoid secondary effects, protein degradation was measured at different time points starting after 1 h and continuing for an additional 3 h period. *A*, expression analysis of *Atg4A*, *Atg4B*, *Atg4C*, and *Atg4D* in fibroblasts from wild-type and *Atg4C*^{-/-} mice. The transcript expression levels are relative to *Atg4C* expression level, which was set at 100%. *B*, the total protein degradation is presented for *Atg4C*^{+/+} (gray bars)- or *Atg4C*^{-/-} (white bars)-derived cells. *C*, the contribution of autophagy to total protein degradation in the presence of 3-methyladenine (3-methyladenine sensitive degradation) under serum, and amino acid deprivation was calculated as previously described (30). These results are taken from four separate experiments with duplicate samples. Four *Atg4C*^{+/+} and five *Atg4C*^{-/-} independent cell lines were used. *D*, the contribution of autophagy to total protein degradation after transfection with *Atg4C*/pCDNA3 or pCDNA3 is presented for *Atg4C*^{+/+}- or *Atg4C*^{-/-}-derived cells under serum and amino acid deprivation.

starved *Atg4C*^{-/-} mice will be very helpful to clarify this question.

In addition to the relevance of autophagy as a physiological response to starvation, this pathway has also been suggested to play an important role in tumor development (52–54). In this regard the activation of several tumor suppressor genes as *Beclin-1*, *p53*, *PTEN*, or *p19ARF* are associated with an up-regulation of autophagy, whereas their loss is often accompanied by a loss of autophagic potential (44, 55–60). On the other hand, several genes which act as oncogenes, including *AKT*, *mTOR*, or *Ras*, are reported inhibitors of autophagy, and their overexpression is associated with a reduced ability of tumor cells to undergo autophagy (52, 61–63). Furthermore, several recent studies have described a protective role for autophagy as an alternative cell death pathway that is activated in cancer cells that have lost their potential to undergo apoptosis (64–66). All these findings suggest that malignant transformation exposes cells to a stressing situation in which all their autophagic potential would be required. Accordingly, a reduction in the ability of inducing autophagy could eventually lead to a higher rate of tumorigenesis under compromising conditions. To test this hypothesis, we examined the susceptibility of *Atg4C*^{-/-}

mice to cancer development with the finding that these mice show a higher incidence of MCA-induced fibrosarcomas, which is consistent with the proposed tumor suppressor role for autophagy processes. Moreover, the fact that *Atg4C* loss leads to a reduced autophagic response in fibroblasts under stressing conditions such as starvation could contribute to explain the higher incidence of fibrosarcomas, which are fibroblast-derived tumors, observed in *Atg4C* mutant mice.

In summary, in this work we show that *Atg4C* activity is not essential for autophagy under normal conditions *in vivo*. However, under demanding conditions such as starvation *Atg4C* disruption leads to a tissue-specific decrease of autophagy in diaphragm, a tissue that is dependent on a continuous and high rate of energy consumption, and also to a reduced resistance to prolonged fasting. In addition, *Atg4C*^{-/-} mice also show a higher incidence of MCA-induced fibrosarcomas as compared with their wild-type littermates, which could be correlated to the decrease in autophagy observed in *Atg4C*-deficient fibroblasts under nutritional stressful conditions. Further studies

involving mice deficient in other components of the *Atg4* proteinase family will help to define the precise *in vivo* role of each family member in both normal and pathological conditions including cancer.

Acknowledgments—We thank F. Rodríguez, M. Fernández, and M. S. Pitiot for excellent technical assistance, Drs. A. M. Pendás, J. M. Freije, X. S. Puente, A. Baamonde, P. Zuazua, A. Astudillo, O. García-Suarez, and G. R. Ordoñez for support and helpful comments, and Dr. T. Ueno (Juntendo University, Tokyo) for providing anti-*Atg4C*, *GATE-16*, *GABARAP*, and *LC3* antibodies. The Instituto Universitario de Oncología is supported by Obra Social Cajastur-Asturias.

REFERENCES

- Mizushima, N. (2005) *Cell Death Differ.* **12**, Suppl. 2, 1535–1541
- Marino, G., and Lopez-Otin, C. (2004) *Cell. Mol. Life Sci.* **61**, 1439–1454
- Klionsky, D. J. (2005) *Curr. Biol.* **15**, 282–283
- Cuervo, A. M. (2004) *Mol. Cell. Biochem.* **263**, 55–72
- Shintani, T., and Klionsky, D. J. (2004) *Science* **306**, 990–995
- Huang, P. H., and Chiang, H. L. (1997) *J. Cell Biol.* **136**, 803–810
- Tsukada, M., and Ohsumi, Y. (1993) *FEBS Lett.* **333**, 169–174
- Thumm, M., Egner, R., Koch, B., Schlumpberger, M., Straub, M., Veenhuis, M., and Wolf, D. H. (1994) *FEBS Lett.* **349**, 275–280
- Huang, W. P., and Klionsky, D. J. (2002) *Cell Struct. Funct.* **27**, 409–420

10. Mizushima, N., Noda, T., Yoshimori, T., Tanaka, Y., Ishii, T., George, M. D., Klionsky, D. J., Ohsumi, M., and Ohsumi, Y. (1998) *Nature* **395**, 395–398
11. Ichimura, Y., Kirisako, T., Takao, T., Satomi, Y., Shimonishi, Y., Ishihara, N., Mizushima, N., Tanida, I., Kominami, E., Ohsumi, M., Noda, T., and Ohsumi, Y. (2000) *Nature* **408**, 488–492
12. Kirisako, T., Ichimura, Y., Okada, H., Kabeya, Y., Mizushima, N., Yoshimori, T., Ohsumi, M., Takao, T., Noda, T., and Ohsumi, Y. (2000) *J. Cell Biol.* **151**, 263–276
13. Kim, J., Huang, W. P., and Klionsky, D. J. (2001) *J. Cell Biol.* **152**, 51–64
14. Lang, T., Schaeffeler, E., Bernreuther, D., Bredschneider, M., Wolf, D. H., and Thumm, M. (1998) *EMBO J.* **17**, 3597–3607
15. Kabeya, Y., Mizushima, N., Ueno, T., Yamamoto, A., Kirisako, T., Noda, T., Kominami, E., Ohsumi, Y., and Yoshimori, T. (2000) *EMBO J.* **19**, 5720–5728
16. Tanida, I., Tanida-Miyake, E., Ueno, T., and Kominami, E. (2001) *J. Biol. Chem.* **276**, 1701–1706
17. Tanida, I., Tanida-Miyake, E., Komatsu, M., Ueno, T., and Kominami, E. (2002) *J. Biol. Chem.* **277**, 13739–13744
18. Mizushima, N., Yoshimori, T., and Ohsumi, Y. (2003) *Int. J. Biochem. Cell Biol.* **35**, 553–561
19. Mizushima, N., Yamamoto, A., Hatano, M., Kobayashi, Y., Kabeya, Y., Suzuki, K., Tokuhiisa, T., Ohsumi, Y., and Yoshimori, T. (2001) *J. Cell Biol.* **152**, 657–668
20. Marino, G., Uria, J. A., Puente, X. S., Quesada, V., Bordallo, J., and Lopez-Otin, C. (2003) *J. Biol. Chem.* **278**, 3671–3678
21. He, H., Dang, Y., Dai, F., Guo, Z., Wu, J., She, X., Pei, Y., Chen, Y., Ling, W., Wu, C., Zhao, S., Liu, J. O., and Yu, L. (2003) *J. Biol. Chem.* **278**, 29278–29287
22. Hemelaar, J., Lelyveld, V. S., Kessler, B. M., and Ploegh, H. L. (2003) *J. Biol. Chem.* **278**, 51841–51850
23. Scherz-Shouval, R., Sagiv, Y., Shorer, H., and Elazar, Z. (2003) *J. Biol. Chem.* **278**, 14053–14058
24. Tanida, I., Sou, Y. S., Ezaki, J., Minematsu-Ikeguchi, N., Ueno, T., and Kominami, E. (2004) *J. Biol. Chem.* **279**, 36268–36276
25. Puente, X. S., Sanchez, L. M., Overall, C. M., and Lopez-Otin, C. (2003) *Nat. Rev. Genet.* **4**, 544–558
26. López-Otín, C., and Overall, C. M. (2002) *Nat. Rev. Mol. Cell Biol.* **3**, 509–519
27. Chomczynski, P., and Sacchi, N. (1987) *Anal. Biochem.* **162**, 156–159
28. Livak, K. J., and Schmittgen, T. D. (2001) *Methods* **25**, 402–408
29. Mizushima, N., Yamamoto, A., Matsui, M., Yoshimori, T., and Ohsumi, Y. (2004) *Mol. Biol. Cell* **15**, 1101–1111
30. Fuertes, G., Villarroja, A., and Knecht, E. (2003) *Int. J. Biochem. Cell Biol.* **35**, 651–664
31. Kaplan, E., and Meier, P. (1958) *J. Am. Stat. Assoc.* **53**, 457–481
32. Kuma, A., Hatano, M., Matsui, M., Yamamoto, A., Nakaya, H., Yoshimori, T., Ohsumi, Y., Tokuhiisa, T., and Mizushima, N. (2004) *Nature* **432**, 1032–1036
33. Komatsu, M., Waguri, S., Ueno, T., Iwata, J., Murata, S., Tanida, I., Ezaki, J., Mizushima, N., Ohsumi, Y., Uchiyama, Y., Kominami, E., Tanaka, K., and Chiba, T. (2005) *J. Cell Biol.* **169**, 425–434
34. Folgueras, A. R., Pendas, A. M., Sanchez, L. M., and Lopez-Otin, C. (2004) *Int. J. Dev. Biol.* **48**, 411–424
35. Kim, T. S., Heinlein, C., Hackman, R. C., and Nelson, P. S. (2006) *Mol. Cell Biol.* **26**, 965–975
36. Weskamp, G., Cai, H., Brodie, T. A., Higashiyama, S., Manova, K., Ludwig, T., and Blobel, C. P. (2002) *Mol. Cell Biol.* **22**, 1537–1544
37. Qu, X., Yu, J., Bhagat, G., Furuya, N., Hibshoosh, H., Troxel, A., Rosen, J., Eskelinen, E. L., Mizushima, N., Ohsumi, Y., Cattoretti, G., and Levine, B. (2003) *J. Clin. Investig.* **112**, 1809–1820
38. Yue, Z., Jin, S., Yang, C., Levine, A. J., and Heintz, N. (2003) *Proc. Natl. Acad. Sci. U. S. A.* **100**, 15077–15082
39. Kabeya, Y., Mizushima, N., Yamamoto, A., Oshitani-Okamoto, S., Ohsumi, Y., and Yoshimori, T. (2004) *J. Cell Sci.* **117**, 2805–2812
40. Kamimoto, T., Shoji, S., Hidvegi, T., Mizushima, N., Umebayashi, K., Perlmutter, D. H., and Yoshimori, T. (2006) *J. Biol. Chem.* **281**, 4467–4476
41. Matsui, M., Yamamoto, A., Kuma, A., Ohsumi, Y., and Mizushima, N. (2006) *Biochem. Biophys. Res. Commun.* **339**, 485–489
42. Manzanedo, C., Aguilar, M. A., Rodriguez-Arias, M., Navarro, M., and Minarro, J. (2004) *Behav. Brain Res.* **150**, 73–82
43. El Yacoubi, M., Bouali, S., Popa, D., Naudon, L., Leroux-Nicollet, L., Hamon, M., Costentin, J., Adrien, J., and Vaugeois, J. M. (2003) *Proc. Natl. Acad. Sci. U. S. A.* **100**, 6227–6232
44. Liang, X. H., Jackson, S., Seaman, M., Brown, K., Kempkes, B., Hibshoosh, H., and Levine, B. (1999) *Nature* **402**, 672–676
45. Schwarze, P. E., and Seglen, P. O. (1985) *Exp. Cell Res.* **157**, 15–28
46. Kisen, G. O., Tessitore, L., Costelli, P., Gordon, P. B., Schwarze, P. E., Baccino, F. M., and Seglen, P. O. (1993) *Carcinogenesis* **14**, 2501–2505
47. Pendas, A. M., Folgueras, A. R., Llano, E., Caterina, J., Frerard, F., Rodriguez, F., Astudillo, A., Noel, A., Birkedal-Hansen, H., and Lopez-Otin, C. (2004) *Mol. Cell Biol.* **24**, 5304–5313
48. Balbin, M., Fueyo, A., Tester, A. M., Pendas, A. M., Pitiot, A. S., Astudillo, A., Overall, C. M., Shapiro, S. D., and Lopez-Otin, C. (2003) *Nat. Genet.* **35**, 252–257
49. Everitt, A. B., Luu, T., Cromer, B., Tierney, M. L., Birnir, B., Olsen, R. W., and Gage, P. W. (2004) *J. Biol. Chem.* **279**, 21701–21706
50. Chen, Z. W., and Olsen, R. W. (2007) *J. Neurochem.* **100**, 279–294
51. Nagler, D. K., and Menard, R. (2003) *Biol. Chem.* **384**, 837–843
52. Kondo, Y., Kanzawa, T., Sawaya, R., and Kondo, S. (2005) *Nat. Rev. Cancer* **5**, 726–734
53. Gozuacik, D., and Kimchi, A. (2004) *Oncogene* **23**, 2891–2906
54. Guertin, D. A., and Sabatini, D. M. (2005) *Trends Mol. Med.* **11**, 353–361
55. Weng, L. P., Smith, W. M., Dahia, P. L., Ziebold, U., Gil, E., Lees, J. A., and Eng, C. (1999) *Cancer Res.* **59**, 5808–5814
56. Liang, C., Feng, P., Ku, B., Dotan, I., Canaani, D., Oh, B. H., and Jung, J. U. (2006) *Nat. Cell Biol.* **8**, 688–699
57. Crighton, D., Wilkinson, S., O'Prey, J., Syed, N., Smith, P., Harrison, P. R., Gasco, M., Garrone, O., Crook, T., and Ryan, K. M. (2006) *Cell* **126**, 121–134
58. Reef, S., Zalckvar, E., Shifman, O., Bialik, S., Sabanay, H., Oren, M., and Kimchi, A. (2006) *Mol. Cell* **22**, 463–475
59. Feng, Z., Zhang, H., Levine, A. J., and Jin, S. (2005) *Proc. Natl. Acad. Sci. U. S. A.* **102**, 8204–8209
60. Ogier-Denis, E., and Codogno, P. (2003) *Biochim. Biophys. Acta* **1603**, 113–128
61. Blume-Jensen, P., and Hunter, T. (2001) *Nature* **411**, 355–365
62. Vivanco, I., and Sawyers, C. L. (2002) *Nat. Rev. Cancer* **2**, 489–501
63. Furuta, S., Hidaka, E., Ogata, A., Yokota, S., and Kamata, T. (2004) *Oncogene* **23**, 3898–3904
64. Cao, C., Subhawong, T., Albert, J. M., Kim, K. W., Geng, L., Sekhar, K. R., Gi, Y. J., and Lu, B. (2006) *Cancer Res.* **66**, 10040–10047
65. Kim, R., Emi, M., and Tanabe, K. (2005) *Oncol. Rep.* **14**, 595–599
66. Kim, R., Emi, M., Tanabe, K., Uchida, Y., and Arihiro, K. (2006) *Eur. J. Surg. Oncol.* **32**, 269–277